сообщения
объединенного
института
ядерных
исследований
дубна

E1-82-286

Z.Strugalski, R.Niszcz*, W.Peryt, J.Pluta*

NEUTRAL PION PRODUCTION IN PION-XENON NUCLEUS COLLISIONS AT 3.5 GeV/c MOMENTUM

* Institute of Physics of the Warsaw Technical University, Warsaw, Poland.

1982

1. INTRODUCTION

The subject matter in this article is to present experimental data on the neutral pion production in pion-xenon nucleus collisions at 3.5 GeV/c momentum.

Neutral pions, if registered with an efficiency of about 100%, as it is met often in experiments with some of the heavy liquid bubble chambers, can serve as effective probes for the particle production process study in hadron-nucleus and hadron-nucleon collisions. They can be registered within total interval of their kinetic energies, including zero MeV. Their kinetic energies and emission angles can be now estimated with an accuracy high enough for the problems under investigations.

In collecting the data on the neutral pions, data on the fast protons emitted, of kinetic energies of about 20-400 MeV, and data on the electrically charged pions produced have been picked up as well; this set provides the information about the correlation between the proton emission and the pion production intensities, i.e., about a dependence of the number of emitted protons on the multiplicity of the charged and neutral pions produced.A large amount of new experimental data has been accumulated, this way, which may provide new information with regard to the neutral pion production process, and about the pion production process at all.

2. EXPERIMENT

The pion-xenon nucleus collision events used for the analysis performed in this paper were registered in the 180 litre xenon bubble chamber [1] exposed to negatively charged pion beam of 3.5 GeV/c momentum, from the accelerator at the Moscow Institute of Theoretical and Experimental Physics.

We omit the detailed description of our experiment; it can be found in our previous works [2,3]. We limit ourselves here only to present the most important information about our experiment.

The xenon bubble chamber of 104x40x43 cm^3 volume works without a magnetic field; it is a 4π geometry detector for

particles emitted from its center, if of kinetic energies: a) 15-220 MeV of protons, b) 0-150 MeV of positively charged pions, c) 10-150 of negatively charged pions; d) larger than 0 MeV, including 0, of neutral pions; within these energy regions the particles can be identified. Particle tracks are detectable in the chamber with a constant efficiency if of the lengths larger than 5 mm, this corresponds to the lower limits of particle kinetic energy written above: for protons and negatively charged pions.

Beam: no more than 5 negatively charged pions per cycle, along the long chamber axis.

Fiducial volume for the interactions: the volume of 42x x10x10 cm^3 located coaxially and centered inside the chamber. The end or deflection point of any beam-pion track were accepted to be the interaction location.

Scanning efficiency for the interaction events is nearly 99%; scanning efficiency for the neutral pions is about 99% as well.

Accuracy of measurements: proton and charged pion energies - by the range-energy relations - about 4% in average; neutral pions - by the total track length method /4/ - about 12% in average. Proton emission angles - about 1 degree.

About 90% of all protons emitted atop inside the chamber, and their energies can be measured.

3. EXPERIMENTAL DATA

A sample of 2800 pion-xenon nucleus collision events with any number of secondaries selected in scanning of 20000 chamber photographs forms the basis of this work; in preparing some of experimental characteristics, additional portion of material, nearly as large as the basic one, has been used as well.

From among these events the classes with any number n_γ = 0,1,2,3,... of registered gamma quanta accompanying the collisions can be distinguished, table 1. Applying the statistical regularization method /5-8/, the corrected numbers of the gamma emitted in fact, were estimated, table 1. The total number of observed gamma quanta is 4900, which amounts, in average, the gamma quanta multiplicity $n_\gamma = 1.80 \pm 0.04$ per event. Taking into account high efficiency of the gamma quantum registration, it follows, from table 1, that ~60% of the collision events are accompanied by the gamma quanta.

Energy spectrum of the gamma quanta accompanying the pion-xenon nucleus collisions is presented in fig.1.

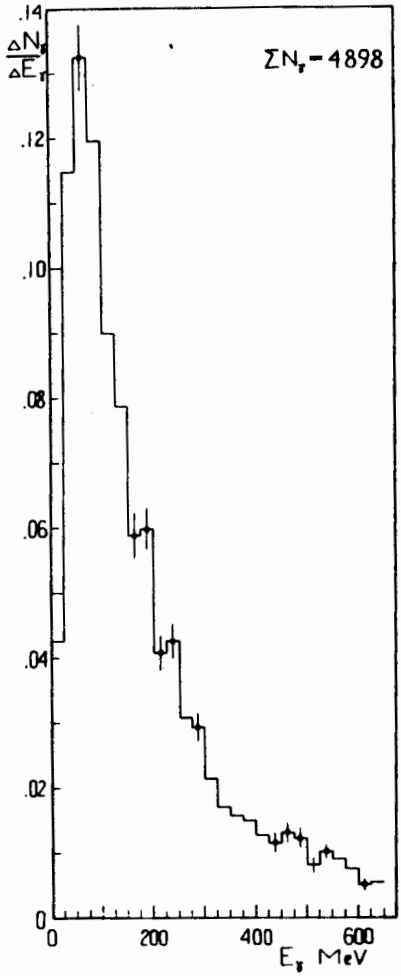

Fig.1. Energy spectrum of the gamma quanta accompanying the pion-xenon nucleus collisions; E_γ - gamma quantum energy, $\frac{\Delta N_\gamma}{\Delta E_\gamma}$ - number of the gamma quanta per 25 MeV, ΣN_γ total number of the gamma quanta included in the histogram.

Fig.2. Distribution of the values of the effective masses $m_{\gamma\gamma}$, Eq. (1), corresponding to the neutral pions and eta mesons.

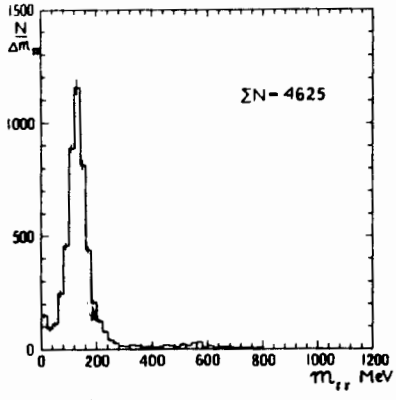

Combinations of the registered gamma quanta in pairs form the effective masses $m_{\gamma_i\gamma_j}$:

$$m^2_{\gamma i \gamma j} = 2E_{\gamma i} E_{\gamma j} (1 - \cos\theta_{\gamma i \gamma j}), \qquad (1)$$

where $E_{\gamma i}$, $E_{\gamma j}$ are the energies of any i-th and j-th two gamma quanta $i \neq j$; $\theta_{\gamma i \gamma j}$ the angle between the emission directions of these quanta. The combination procedure is described in our former works [9,10]. The effective mass $m_{\gamma\gamma}$ distribution in the total sample of $m_{\gamma\gamma}$ values satisfying the accepted for the neutral pion and for the eta meson, in accordance with the measurement accuracy [9,10], is shown in fig.2.

Table 1

Gamma quanta multiplicity, n_γ, distribution in the pion-xenon nucleus collision events. $N(n_\gamma)$ -number of events with the gamma quanta multiplicity n_γ

n_γ	Observed		Corrected
	$N(n_\gamma)$	$\pm \Delta N(n_\gamma)$	$N(n_\gamma)$
0	1110	33.3	1123
1	145	12.0	0
2	872	29.5	989
3	113	10.6	0
4	366	19.1	483
5	36	6.0	0
6	86	9.8	138
7	12	3.5	0
8	37	6.1	37
9	4	2.0	0
10	8	2.8	10
11	0	0	0
12	1	1	16

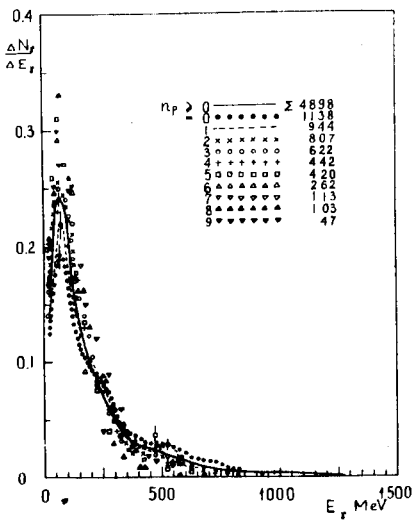

Fig.3. Energy spectra of the gamma quanta accompanying the pion-xenon nucleus collisions with various multiplicities n_p of protons emitted; $\frac{\Delta N_\gamma}{\Delta E_\gamma}$ - number of gamma quanta per 50 MeV, E_γ - the energy of gamma quantum.

It can be concluded that observed gamma quanta are predominantly from the neutral pion decays; a small portion of the gamma quanta is from the eta decays, fig.2. It is known,

however, that a small portion of the total sample of gamma quanta is from the omega zero particle decays [9-13], but it influences not remarkably the shape of the gamma quanta energy spectrum. In result of our observations, in investigating the gamma quanta emission process [9-13], the gamma quanta sources such as eta and omega zero manifest themselves predominantly in the class of the quasi-elementary pion-nucleon collisions of incident pions with the periphery of the target nucleus.

We found to be useful to present the characteristics both of the gamma quanta emission and of the neutral pions production. A comparison of appropriate characteristics may provide valuable indications concerning the method of the neutral pion investigations by means of small efficiency gamma quanta detectors.

In figs.3-5 the proton multiplicity dependences of the energy spectra, longitudinal and transverse momenta distributions of the gamma quanta are presented. In fig.6 average values of the energy, longitudinal momentum, transverse momentum of gamma quanta dependending or the proton multiplicity are shown.

Let us present now various characteristics of produced neutral pions. We start with the presentation of the neutral pion multiplicity n_{π^0} distribution, fig.7. The proton multiplicity dependence of the neutral pion multiplicity distributions is presented in fig.8. The average neutral pion multiplicity, n_{π^0}, n_p - dependence is shown in fig.9.

Energy spectra of the neutral pions ejected into forward hemisphere, when $\cos\theta_{\pi^0} > 0$, and into backward hemisphere, $\cos\theta_{\pi^0} < 0$, are presented in fig.10. The n_p-dependence of the neutral pion energy spectrum, for pions ejected in any direction, is shown in fig.11. In this figure the spectra for the classes with the proton multiplicities $n_p \geq 0$, $n_p = 0$, 1,4,8 are presented only; the spectra for the n_p values 2,3,5, 6 are similar.

Distributions of the longitudinal and transverse momenta of the neutral pions, $P_{\parallel \pi^0}$ and $P_{\perp \pi^0}$, are shown in figs.12 and 13, in the classes of events with various proton multiplicity.

Distributions of the neutral pion emission angles, θ_{π^0}, in the classes of events with various proton multiplicities, are shown in fig.14.

The n_p-dependences of the average kinetic energy, $\bar{E}_{k\pi^0}$, average longitudinal momentum, $\bar{P}_{\parallel \pi^0}$, and average transverse mo-

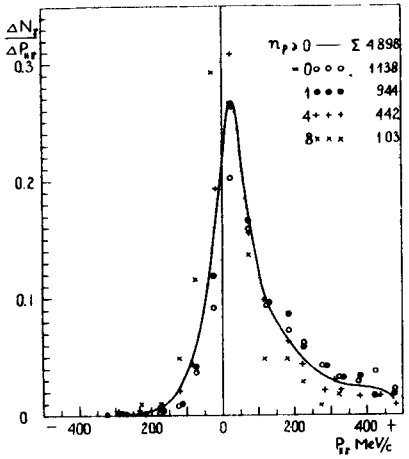

Fig.4. Longitudinal momentum, $P_{\parallel\gamma}$, distributions in pion-xenon nucleus collision events with various numbers n_p of the protons emitted; $\frac{\Delta N_\gamma}{\Delta P_{\parallel\gamma}}$ - number of gamma quanta per 50 MeV/c; solid line - best fit at $n_p \geq 0$.

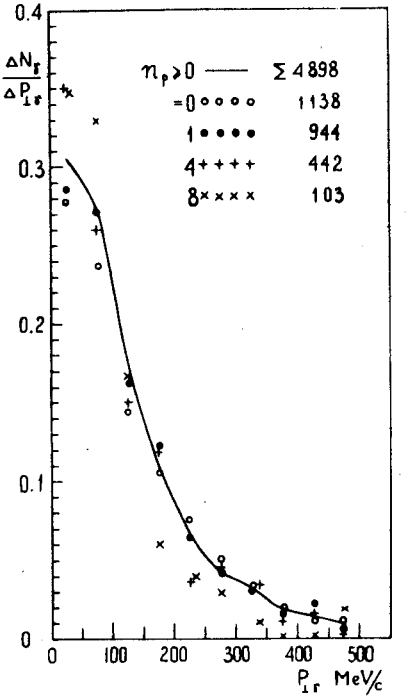

Fig.5. Transverse momentum, $P_{\perp\gamma}$, of emitted gamma quanta in dependence on the multiplicities n_p of emitted protons; $\frac{\Delta N_\gamma}{\Delta P_{\perp\gamma}}$ - number of gamma quanta per momentum interval of 50 MeV/c; solid line - best fit to the distribution for events with $n_p \geq 0$.

Fig.6. Average energy, $\bar{E}_\gamma$, average longitudinal momentum, $\bar{P}_{\gamma\parallel}$, average transverse momentum, $\bar{P}_{\gamma\perp}$, distributions of the gamma quanta emitted in pion-xenon nucleus collisions with various multiplicities n_p of emitted protons.

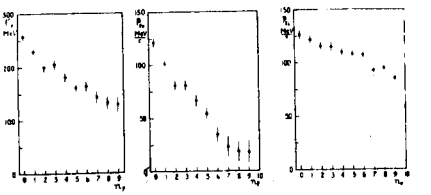

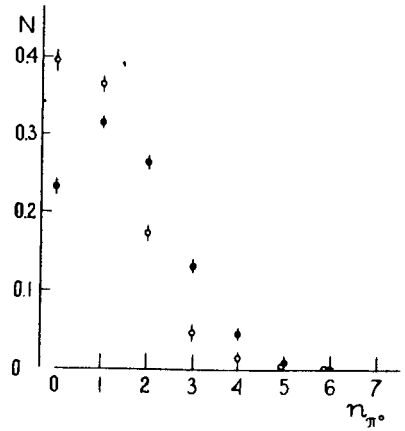

Fig.7. Neutral pion multiplicity, n_{π^0}, distribution in pion-xenon nucleus collisions at 3.5 GeV/c; empty circles - experiment, full circles - predictions given by the intranuclear cascade model.

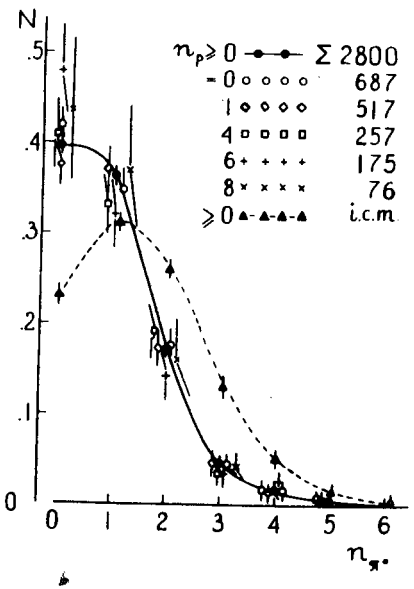

Fig.8. Neutral pion multiplicity, n_{π^0}, distributions in the classes of the pion-xenon collision events with various proton multiplicity, n_p; --▲-- predictions given by the intranuclear cascade model for the class of events with $n_p \geq 0$, N - number of events with the number n_{π^0} of produced pions.

Fig.9. The proton multiplicity dependence, n_p - dependence, of the average neutral pion multiplicity, $< n_{\pi^0} >$, in pion-xenon collision events; ● - experiment, o - predictions of the intranuclear cascade model, × - predictions given by the model of Strugalski[17]; solid lines - best fits to the predictions and to the experimental data correspondingly.

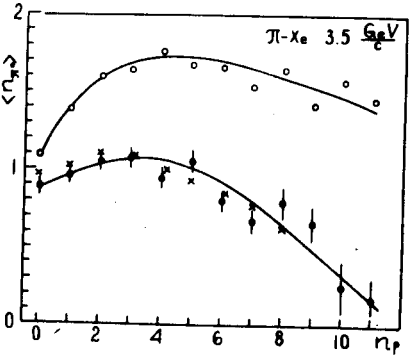

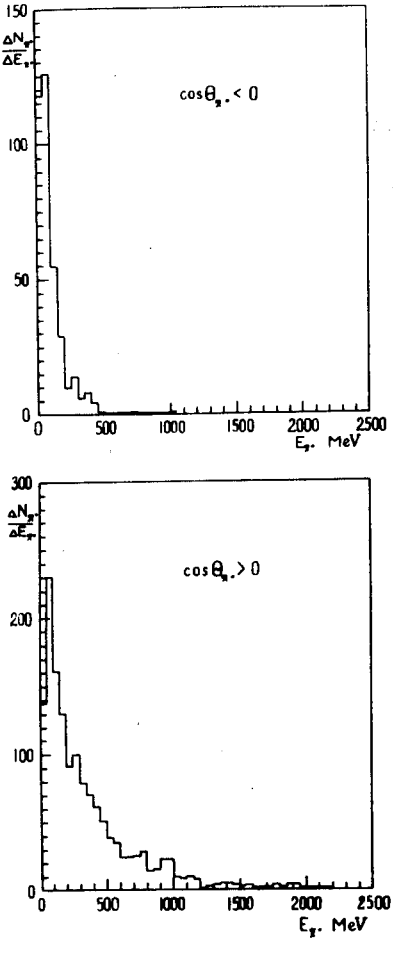

Fig. 10. Energy spectra of the neutral pions ejected into forward and into backward hemispheres; E_{π^0} - pion energy, $\frac{\Delta N_{\pi^0}}{\Delta E_{\pi^0}}$ - number of pions per 50 MeV, θ_{π^0} - pion emission angle.

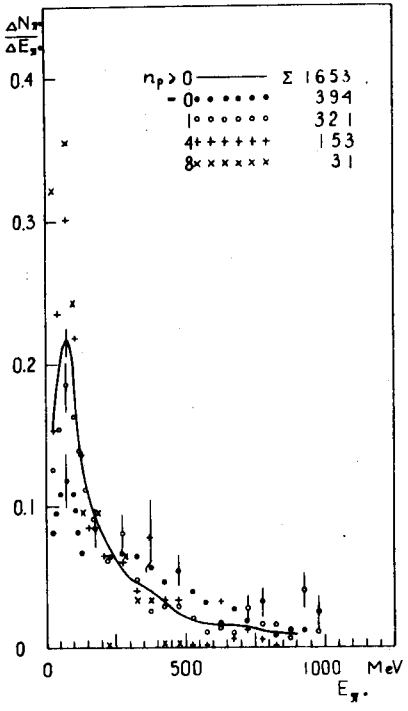

Fig. 11. Energy spectra of neutral pions produced in pion-xenon nucleus collisions with various multiplicities n_p of emitted protons; E_{π^0} - energy of pions, $\frac{\Delta N_{\pi^0}}{\Delta E_{\pi^0}}$ - number of pions per 50 MeV/c.

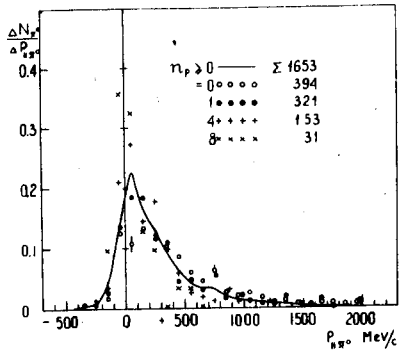

Fig.12. Longitudinal momentum, $P_{\parallel\pi^0}$, distributions of neutral pions produced in pion-xenon nucleus collisions with various multiplicities n_p of emitted protons; $\frac{\Delta N_{\pi^0}}{\Delta P_{\parallel\pi^0}}$ - number of pions per 100 MeV/c.

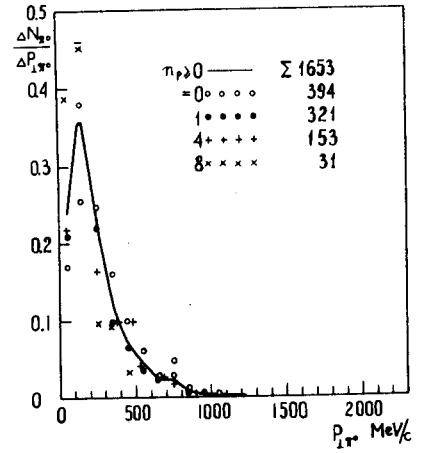

Fig.13. Neutral pion transverse momentum, $P_{\perp\pi^0}$, distributions in pion-xenon nucleus collisions with various multiplicities n_p of emitted protons; $\frac{\Delta N_{\pi^0}}{\Delta P_{\perp\pi^0}}$ - numbers of neutral pions per 100 MeV/c.

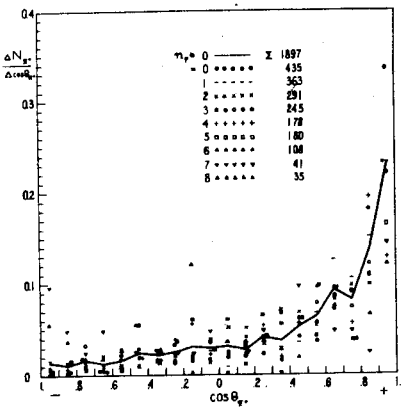

Fig.14. Neutral pion emission angle distributions in pion-xenon nucleus collision events with various proton multiplicities n_p; $\frac{\Delta N_{\pi^0}}{\cos\theta_{\pi^0}}$ numbers of neutral pions per 0.1 of the cosine of the emission angle θ_{π^0}.

mentum, $\bar{P}_{\perp\pi^0}$, of produced neutral pions are presented in fig.15.

After presentation of various characteristics of the neutral pions we come now to a short analysis of the relation between the n_p-dependences of the neutral pion multiplicity and the multiplicity of the electrically charged pions. We introduce following quantity:

$$\kappa(n_p) = \frac{N_{\pi^0}}{(N_{\pi^0} + N_{\pi^+} + N_{\pi^-})}, \qquad (2)$$

where N_{π^0}, N_{π^+}, N_{π^-} are the numbers of pions - neutral, positively and negatively charged - produced in the class of events with a given multiplicity, n_p, of emitted protons;

Fig. 15. Proton multiplicity dependences, n_p - dependences, of the average kinetic energy, $\bar{E}_{k\pi^0}$, average longitudinal momentum, $\bar{P}_{\parallel\pi^0}$, and average transverse momentum, $\bar{P}_{\perp\pi^0}$, of the neutral pions produced in pion-xenon nucleus collisions.

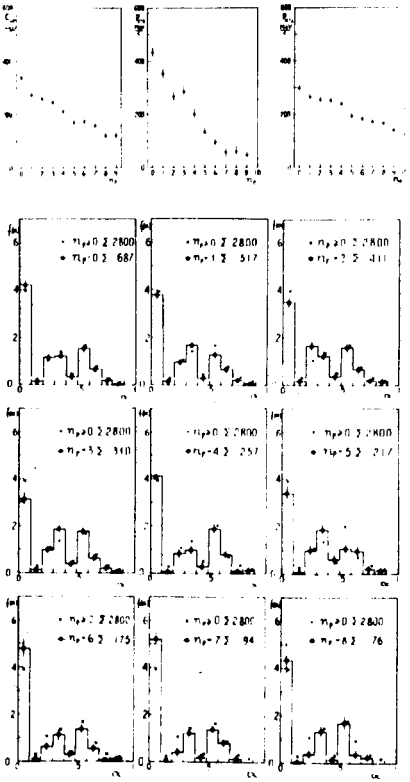

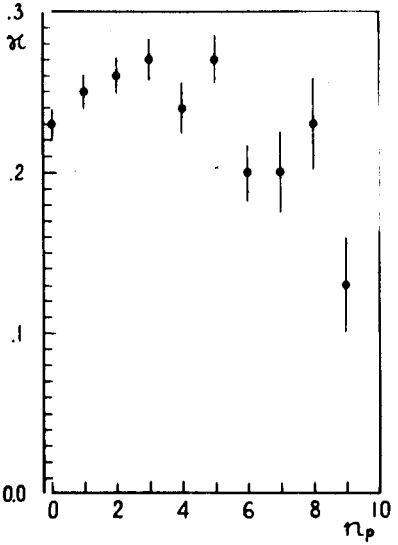

Fig. 16. The n_p-dependence of the average value $\langle\kappa\rangle$ of the quantity κ, Eq. (2).

Fig. 17. The $f(\alpha \equiv \kappa)$ distributions in classes of the pion-xenon nucleus collision events with various proton multiplicity n_p; $\alpha \equiv \kappa = N_{\pi^0}/N_{\pi} = N_{\pi^0}/(N_{\pi^0} + N_{\pi^+} + N_{\pi^-})$, where N_{π} are the numbers of produced pions of any charge, and $N_{\pi^0} = 0, 1, 2, \ldots$, in events with a given proton multiplicity n_p.

N_{π^0} can be 0,1,2,3,... . The n_p-dependence of the average values of $\langle\kappa\rangle$ is shown in fig.16; in fig.17 the distributions of the $f(a) \equiv f(\kappa)$ in the classes of events with various proton multiplicities are presented. It is seen, from fig. 16, that the number of produced neutral pions amounts no more than 0.3 of the total number of all the pions produced. It follows from fig.17 that the charged pion multiplicity distribution n_p-dependence is the same, on the average, as that of the neutral pions.

4. DATA ANALYSIS

The subject matter in this section is an analysis of the experimental data, on the neutral pion production mainly, presented above. However, the results of this analysis will concern the pion production in general as well - not only the neutral ones; it is reasonable to think the characteristics of the electrically charged pions do not differ by much from the characteristics of the neutral pions, as it follows from the data presented in fig.17, for example. The only difference in this experiment is between the information about the neutral pions and about the electrically charged ones - the neutral pions are registered with almost 100% efficiency within the total interval of their energy values, including zero MeV, and it is possible to measure the energies of almost all these pions.

As is usually practiced, physicists confront their experimental results to appropriate predictions provided by any of existing models. In the case, it is reasonable to apply the so-called intranuclear cascade model [14,15]. The opinion is often met that this model describes well the hadron-nucleus collision data at the projectile energies of a few GeV, i.e., just as in our experiment. The calculations, within the frames of this model, has been performed taking into account the experimental conditions in the bubble chamber used in the experiment [8,16]. The predictions could be called "the predictions given by the intranuclear cascade model adapted for the experiment performed with the 180 litre xenon bubble chamber", and it may be stated these predictions to be just testable by our experiment [16].

Before to start the comparison between some data and the predictions, let us first sum up the general features of the experimental characteristics of the pion-nucleus collision presented in section 3. In result of the review of these characteristics, we can conclude:

Table 2

Mean and r.m.s. values for the neutral pion and gamma quantum transverse momentum, $P_{T\pi^o}$ and $P_{T\gamma}$, distributions in the classes of events with various proton multiplicities n_p.

n_p	$\geqslant 0$	0	1	2	3	4	5	6	7	8	$\geqslant 9$
$P_{T\pi^o}$ MeV/c	250	298	266	254	253	238	193	182	171	167	141
r.m.s.	214	238	233	206	233	192	145	125	153	115	120
$P_{T\gamma}$ MeV/c	116	125	122	116	115	111	109	109	93	95	86
r.m.s.	100	104	103	101	96	93	95	96	67	90	60

Table 3

Average and r.m.s. values of the neutral pion angular distributions in dependence on the proton multiplicity n_p; θ_{π^o} - neutral pion emission angle.

n_p	$\geqslant 0$	0	1	2	3	4	5	6	7	8
$\langle\cos\vartheta_{\pi^o}\rangle$	0.4694	0.6224	0.5456	0.4986	0.4493	0.4427	0.3340	0.1370	0.1190	0.150
r.m.s.	0.5140	0.4327	0.4705	0.4691	0.5167	0.4886	0.5330	0.6070	0.6590	0.537

1. The neutral pion multiplicity distribution in the total sample of events, with any multiplicity of the emitted protons, is almost the same as such distributions in the classes of events with $n_p=0,1,2,\ldots$ separately, fig.8.
2. The neutral pion average multiplicity depends weakly on the multiplicity of emitted protons up to $n_p \leq 8$, fig.9; starting from $\langle n_{\pi^o} \rangle \approx 0.9$ at $n_p=0$ it increases with increasing n_p to its maximum value $\langle n_{\pi^o} \rangle \approx 1.05$ at $n_p=3$ and decreases with increasing n_p to $\langle n_{\pi^o} \rangle \approx 0.8$ at $n_p=8$.
3. Maximum value of the neutral pion transverse momentum lies within the interval 100-200 MeV/c; the location of this maximum does not depend on the multiplicity of the emitted protons, fig.13. The mean values for the transverse momentum distributions in the classes of events with various proton multiplicities are given in table 2; for a comparison appropriate data for the gamma quanta are presented in this table as well.
4. The angular distributions of the neutral pions, $\cos\theta_{\pi^o}$, depend on the number of emitted protons fig.14. This dependence is characterized by the data on the average and r.m.s. values given in table 3.
5. Distributions $f(\kappa)$ of the ratio $\kappa = N_{\pi^o}/(N_{\pi^o} + N_{\pi^+} + N_{\pi^-})$ between the number $N_{\pi^o}=0,1,2,\ldots$ of produced neutral pions and the number $N_\pi = N_{\pi^o} + N_{\pi^+} + N_{\pi^-}$ of produced pions of any electric charge do not depend on the proton multiplicity n_p, fig.17.

Let us compare now some of the characteristics of the neutral pion production with corresponding predictions given by the intranuclear cascade model. We restrict ourselves to the comparison of the neutral pion multiplicity distributions, figs.7 and 8, and of the neutral pion average multiplicity $\langle n_{\pi^o} \rangle$ n_p-dependence, fig.9. The last characteristic is compared with the prediction given by the model proposed by Z. Strugalski [17] as well.

The comparisons of the distributions of the kinetic energy, of emission angles, and of the n_p-dependences of the average transverse momentum of the neutral pions with appropriate predictions given by the intranuclear cascade model are presented in our former paper [18].

5. COCLUSION

In result of the comparisons presented in foregoing section, it can be stated that: 1. The experimentally determined neutral pion multiplicity distribution does not agree with the predicted one, figs.7 and 8; 2. The experimentally determined

n_p -dependence of the average neutral pion multiplicity $<n_{\pi^0}>$ does not agree with the predicted one, fig.9.

It is known, as well, that the predicted n_p -dependence of the multiplicity n_π of the pions produced (of any charge), disagrees by much with the experimental one [16].

But, we know that many of characteristics of the pion-xenon nucleus collision process are reproduced by the intranuclear cascade model well enough [16].

REFERENCES

1. Kusnetsov E. et al. Instrumentation and Experimental Technique, (Russian PTE), 1970, 2, p. 56.
2. Strugalski Z. et al. JINR, E1-80-39, Dubna, 1980.
3. Strugalski Z. et al. JINR, E1-81-578, Dubna, 1981.
4. Strugalski Z. JINR, 796, Dubna, 1961; Konovalova L.P. Okhrimenko L.S., Strugalski Z. Instrumentation and Experimental Technique (Russian PTE), 1961, 6, p. 26; Ivanovskaya I.A. et al. PTE, 1968, 2, p. 39; Strugalski Z. JINR, P13-6406, Dubna, 1972. 2, p. 39; Strugalski Z. JINR, P13-6406, Dubna, 1972.
5. Turchin V.F. Journ. of Computational Math. and Physics (Russian), 1968, 8, p. 230.
6. Turchin V.F., Kozlov V.P., Malkevich M.I. Uspekhi Fiz. Nauk, 1970, 102, p. 345.
7. Turchin V.F., Nozik V.Z. Phys. of Atmosphere and Ocean, 1969, 1, p. 29.
8. Peryt W. PhD Theses, Warsaw Technical University, Warsaw, Poland, 1979.
9. Strugalski Z. et al. JINR, E1-5349, Dubna, 1970.
10. Strugalski Z. et al. Nuclear Phys., 1971, B27, p. 429.
11. Okhrimenko L.S.. et al. JINR, E1-11054, Dubna, 1977.
12. Abrosimov A.T. et al. Journ. of Nucl.Phys. (Russian), 1980, 2, p. 371.
13. Abrosimov A.T. et al. JINR, R1-12848, Dubna, 1979.
14. Barashenkov V.S., Toneev V.D. Interactions of High Energy Particles and Nuclei with Nuclei, Atomizdat, Moscow, 1972.
15. Barashenkov V.S., Gudima K.K., Toneev V.D. Acta Physica Polonica, 1969, 36, p. 415, 457, 887.
16. Peryt W. et al. JINR, E1-81-803, Dubna, 1981.
17. Strugalski Z. JINR, E1-81-154; E1-81-155; E1-81-156, Dubna, 1981.

Received by Publishing Department
on April 15 1982.